Preliminary Assessment of a Postural Synergy-Based Exoskeleton for Post-Stroke Upper Limb Rehabilitation

Chang He, Cai-Hua Xiong, *Member, IEEE*, Ze-Jian Chen, Wei Fan, Xiao-Lin Huang, and Chenglong Fu, *Member, IEEE*

***Abstract*— Upper limb exoskeletons have drawn significant attention in neurorehabilitation because of the anthropomorphic mechanical structure analogous to human anatomy. Whereas, the training movements are typically unorganized because most exoskeletons ignore the natural movement characteristic of human upper limbs, particularly inter-joint postural synergy. This paper introduces a newly developed exoskeleton (Armule) for upper limb rehabilitation with a postural synergy design concept, which can reproduce activities of daily living (ADL) motion with the characteristics of human natural movements. The semi-transparent active control strategy with the interactive force guidance and visual feedback ensured the active participation of users. Eight participants with hemiplegia due to a first-ever, unilateral stroke were recruited and included. They participated in exoskeleton therapy sessions for 4 weeks, with passive/active training under trajectories and postures with the characteristics of human natural movements. The primary outcome was the Fugl-Meyer Assessment for Upper Extremities (FMA-UE). The secondary outcomes were the Action Research Arm Test(ARAT), modified Barthel Index (mBI), and metric measured with the exoskeleton After the 4-weeks intervention, all subjects showed significant improvements in the following clinical measures: the FMA-UE (difference, 11.50 points, $p = 0.002$), the ARAT (difference, 7.75 points $p < 0.001$), and the mBI (difference, 17.50 points, $p = 0.003$) score. Besides, all subjects showed significant improvements in kinematic and interaction force metrics measured with the exoskeleton. These preliminary results demonstrate that the Armule exoskeleton could improve individuals' motor control and ADL function after stroke, which might be associated with kinematic and interaction force optimization and postural synergy modification during functional tasks.**

***Index Terms*— Postural synergy, exoskeleton, upper limb, rehabilitation robotics.**

I. Introduction

STROKE is the leading cause of adult mortality and disability worldwide [1], and more than two-thirds of stroke survivors arrive at the hospital with motor impairments and function in the upper limbs characterized by muscle weakness, spasms, loss of coordination, and pathological synergies. Also, upper limb dysfunction leads to long-term limitation in ADL and social participation which dysfunction severely affecting the quality of life in stroke survivors and bringing great domestic and socioeconomic burden.

Motor relearning theories are often used to guide stroke rehabilitation [2], which requires training of movement components and integrated functional practice [3] under the mechanism of use-dependent plasticity [4] and operant reinforcement processes [5]–[8]. However, the traditional rehabilitation training method is not only time-consuming and laborious but also can not accurately reproduce the characteristics of human natural movements.

Robot-assisted training is an innovative exercise-based therapy that involves the principles of motor learning. It lightens the burden on the therapist and can provide highly intensive, adaptive, and task-specific training as well as feedback and motivation for enhancing neuroplasticity, more importantly, it introduces a standardized quantitative evaluation method for the rehabilitation training process. Over the last decades, various robotic devices with different training modalities, structures, and principles have been developed for upper-limb training after stroke. Among them, the exoskeleton rehabilitation robot, due to its humanoid structure matching with the upper limb and the ability to apply quantified torque to each specific joint, has been widely concerned [9]. Most upper limb exoskeletons have more than five degree of freedom (DOF) for shoulder, elbow, and wrist movements so that they can

Manuscript received January 30, 2021; revised April 27, 2021 and June 24, 2021; accepted August 20, 2021. Date of publication August 24, 2021; date of current version September 10, 2021. This work was supported in part by the National Natural Science Foundation of China under Grant 52027806, Grant 52005191, Grant U1911601, Grant 52075191, and Grant U1913205 and in part by Hubei Provincial Natural Science Foundation under Grant 2020CFB424. *(Corresponding author: Cai-Hua Xiong.)*

This work involved human subjects or animals in its research. Approval of all ethical and experimental procedures and protocols was granted by the Clinical Trials Ethics Committee of Huazhong University of Science and Technology under Application No. IRB [2018]-235.

Chang He and Cai-Hua Xiong are with the State Key Laboratory of Digital Manufacturing Equipment and Technology, School of Mechanical Science and Engineering, Huazhong University of Science and Technology, Wuhan, Hubei 430074, China (e-mail: chxiong@hust.edu.cn).

Ze-Jian Chen, Wei Fan, and Xiao-Lin Huang are with the Department of Rehabilitation Medicine, Tongji Hospital, Tongji Medical College, Huazhong University of Science and Technology, Wuhan, Hubei 430074, China.

Chenglong Fu is with the Department of Mechanical and Energy Engineering, Southern University of Science and Technology, Shenzhen 518055, China.

Digital Object Identifier 10.1109/TNSRE.2021.3107376

adapt to the human upper limb [10], which has superior motor control; some examples include ABLE [11] ALEx [12], L-Exos [13], CADEN-7 [14], ARMin-V [15], Harmony [16], MGA [17], LIMPACT [18] and ANYexo [19]. Although exoskeleton robots provide a rich range of functional movements, the curse of dimensionality caused by the mechanical structure with a high DOF brings serious challenges to the control strategy [20]. Such a structure also means high manufacturing and use costs, making it less cost-effective, which is not conducive to the promotion of rehabilitation robots. In addition, the benefits compared with traditional methods are controversial in terms of functional performance, especially in movement quality and independence in ADL [29]. Therefore, how to optimize the design and training methods of upper limb robots to relearn natural human movements in ADL [30] remains important for researchers to determine.

To complete specific training tasks, especially ADL tasks, most robots need to generate a joint reference trajectory in a high dimensional space [9] to drive the robot directly or serve as a reference for other control strategies. The joint reference trajectories can be exploited from the recordings of movements in healthy subjects or informed by a therapist, but the types of training tasks are limited [21]. The joint reference trajectories can also be computed by an optimal trajectory planner or other motion planners. However, as the laws of human upper limb movement are still unclear [22], the reference trajectory generated by the optimization method or other motion planners does not fully reproduce the natural human movements, which makes the training movements unnatural and even causing joint strain or soft tissue contusion in patients [23].

To encourage patients to participate in exoskeleton training actively, some exoskeleton robots use electromyography [24], electroencephalograph [25], and other electrophysiological tools [26] to drive the rehabilitation robot according to the patient's intention. Nevertheless, the process of decoding electrophysiological signals is exceptionally complicated, with a low success rate and accuracy due to the high-dimensional input and output signals [27]. As a result, a lot of exoskeleton robots adopt control strategies based on human-robot physical interactions [28], such as assist-as-needed, impedance control, and admittance control. All of these strategies should improve the *transparency* of control to the greatest extent possible [29]; that is, the robot must interfere with the patient's autonomous movement as little as possible. Although robots with high transparency can encourage the patient to participate in the training actively [30], they amplify the abnormality of patients' postures and compensatory movements [31]. High transparency also increases the complexity of the structure and control of the exoskeleton [32].

Bernstein's theory of motor control suggested that human motions are quite stereotyped and that motor synergy patterns are common among all humans [33]. Synergy is characterized by the relationship between kinematics, dynamics, or other physiological parameters sharing the same spatial-temporal properties [34]. According to this theory, if the synergies of the human upper limb for specific tasks can be identified, they can be used to reconstruct the natural human movement of the upper limb [35]–[37]. The synergies are usually expressed at muscular and kinematic levels. Several pilot studies have employed synergies at the muscle level to evaluate the changes in muscle synergies after stroke [38], [39] and included synergies as outcome measures to evaluate stroke recovery [40], [41]. Kinematic synergy, including postural synergy and velocities synergy, can be directly used in the reconstruction of natural human movement in applications such as the mechanical structure design and motion planning for artificial limbs/rehabilitation robots [11], [35], [42], [43]. Based on velocity synergy, Crocher *et al.* [44] developed a controller for the upper limb exoskeleton, which can impose a specific velocity synergy constraint on patients during rehabilitation. Hassan *et al.* [45] achieved postural synergy at the control level for gait reconstruction of the lower limb exoskeleton. Some recent studies have shown that postural synergies can improve the efficiency of motor learning in healthy people [46], [47]. Although the design based on postural synergy may limit the overall capacity of the device and cause constraints, by limiting the reproduced tasks to ADL tasks and improving the design of the structure or controller, the human natural motion characteristics can be reproduced to the greatest extent, furthermore, since most stroke survivors exhibit pathological synergies, postural synergy-based rehabilitation robots may help overcome pathological synergies or compensatory motion, allowing patients to relearn normal characteristics of natural human movements [44]. This is exactly in line with the philosophy of classic Bobath therapy [48]. Another important point to note is, by integrating the postural synergy into the exoskeleton mechanical structure allows to simplify its design and construction, could be an effective cost reduction in manufacturing and use [42]. Posture synergies show great potential in the field of rehabilitation. Unfortunately, to the authors' knowledge, currently, no such postural synergy-based upper limb rehabilitation exoskeletons are used in clinical practice.

Aiming to meet the above clinical needs for rehabilitation exoskeletons and overcome the existing problems in the structure and control strategy of rehabilitation exoskeletons, we developed a postural synergy-based rehabilitation exoskeleton [42] with passive/active training control strategies. By integrating the postural synergy into the exoskeleton mechanical structure, allows simplifying its design and construction, reducing its cost. The active training strategy guided the rehabilitation exoskeleton to perform the exercise training with the characteristics of human natural movement in the synergy dimension reduction subspace by using interaction force and visual feedback.

Overall, the main contribution of this paper is:

1) To the best of our knowledge, this is the first clinical trial of an upper exoskeleton that integrates postural coordination into the mechanical structure for the rehabilitation of patients with chronic stroke.
2) A new semitransparent active control strategy with visual feedback was proposed. It enables the exoskeleton to recognize the patient's active motion intentions and provide movement assistance in the synergistic dimension-reducing subspace.

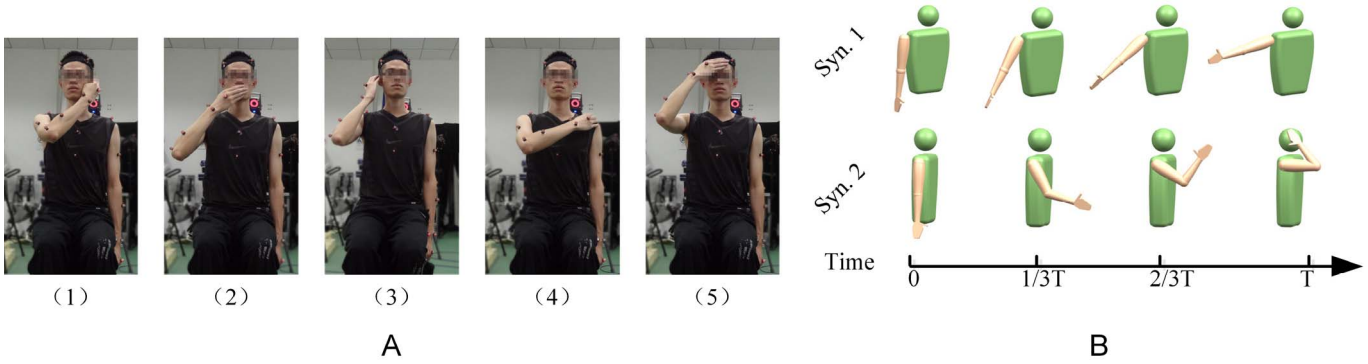

Fig. 1. A (1-5) The five types of natural reaching movements selected in the data collection experiment. (1) Final posture of touching the left ear; (2) Final posture of touching the mouth; (3) Final posture of touching the right ear; (4) Final posture of touching the left shoulder; (5) Final posture of touching the vertex. Fig. 1 B Two most significant postural synergies of the five natural reaching movements. After cluster analysis of the motion data of five kinematic joints, principal component analysis was carried out for each cluster. In cluster one, Syn 1. was extracted to generate the motion of SIER and SAA joints, which can account for more than 97.43% of the variation. In cluster two, Syn 2. was extracted to generate the motion of SFE, EFE and ESP joints, which can account for more than 84.91% of the variation.

3) Preliminary clinical results suggest that training with our robot may improve upper limb motor function.

In the following text, we will describe the mechanical design and control strategies of the exoskeleton, as well as the preliminary evaluation and testing.

II. Methods

A. Exoskeleton Design

In previous work, the natural human movements of upper-limbs are analyzed by the principal component analysis (PCA) method and two most significant synergies of upper-limb movements during five natural reaching movements (including touching the left ear, touching the mouth, touching the right ear, touching the left shoulder and touching the vertex) organized in a dataset that comprised ten subjects, which can account for more than 80% of the variation, are extracted (as shown in Fig. 1). The reason for choosing these natural reaching movements is that these movements involve the shoulder and elbow complex and provide effective stimulation to the major muscles responsible for the motion of the affected limb, such as pectoralis major, biceps brachii, and triceps brachii *et al.*; more crucial is that these movements should be important for the patient to regain the self-care ability of daily living. We propose a postural synergy-based method to design the kinematic transmission mechanism for a multi-joint upper-limb exoskeletal rehabilitation robot with two actuators [42].

Specifically, all of the subjects were requested to finish five natural reaching movements, meanwhile, the five joint angles of the subjects' upper limbs(3 DOFs in the shoulder complex-flexion/extension (SFE), abduction/adduction (SAA), and internal/external rotation (SIER), 2 DOFs in the elbow complex-flexion/extension (EFE) and supination/pronation (ESP))were calculated and recorded by the motion capture system (VICON UK. Ltd). The motion sequence of joint angles is denoted as: $\boldsymbol{\theta} = [\boldsymbol{\theta}_1, \ldots, \boldsymbol{\theta}_t] \in \mathbb{R}^{5\times T}, \boldsymbol{\theta}_t = \left[q_{1,\mathrm{t}}, \ldots, q_{5,\mathrm{t}}\right]^{\mathrm{T}} \in \mathbb{R}^5$, where $q_{n,t}$ is n^{th} joint angle at the t^{th} sampling point $t = 1, \ldots, \mathrm{T}$. PCA method was used to analyze the motion sequence. The configuration of the arm at the tth sampling point can be represented by a vector:

$$\boldsymbol{\theta}_t \approx \overline{\boldsymbol{\theta}} + \boldsymbol{C}\boldsymbol{u}_t \tag{1}$$

where $\boldsymbol{u}_t = \left[u_{1,t}, u_{2,t}\right]^T \in \mathbb{R}^2$, $u_{1,t}, u_{2,t}$ are the positions of the two actuators at the t^{th} sampling point, respectively. $\overline{\boldsymbol{\theta}} \in \mathbb{R}^5$ is the biased vector from the zero position and $\boldsymbol{C} \in \mathbb{R}^{5\times 2}$ is the coupling matrix, and it indicates the linear relation between the angular displacements of the joints. $\boldsymbol{C}$ contains the natural human movement characteristics of these ADL movements. In previous works, we used the method of cluster synergy analysis to obtain $\boldsymbol{C}$ (as shown in Fig. 1 B), and the composition of it is expounded in more detail [42], [49]. The natural motion characteristics of human upper limbs can be reproduced by using appropriate mechanical structures to realize the coupling matrix $\boldsymbol{C}$. In other words, human motion characteristics are embedded into the structure of the robot, making the motion generated by the robot have human-like characteristics. Besides, it is worth mentioning that using this method reduces the number of exoskeleton robot actuators and reduces the cost. To reflect the linear relationship between the angular displacements of each joint contained in $\boldsymbol{C}$, we designed two sets of pulley mechanisms to distribute the actuators' power and motion to each joint in a specific proportion through their transmission ratio settings [42].

Based on this idea, we developed the Armule rehabilitation exoskeletal robot, which has 5 DOF driven by two actuators and the attached coupling kinematic transmission mechanism. The mechanical structure design is embedded with the postural synergies of functional movements, enabling the robot to reconstruct natural human reaching movements inherently (as shown in Fig. 2 A). Specifically, $\boldsymbol{C}$ is denoted as: $C = \begin{bmatrix} \frac{r_0}{r_1} & \frac{r_0 r_2}{r_1 r_3} & 0 & 0 & 0 \\ 0 & 0 & \frac{r_0}{r_4} & \frac{r_0 r_5}{r_4 r_6} & \frac{r_0 r_5 r_7}{r_4 r_6 r_8} \end{bmatrix}^{\mathrm{T}}$, where r_0 is the radius of actuators output pulley, $r_1 - r_8$ are radii of each coupling pulley as shown in Fig. 2 B, C.

Several changes relative to the previous mechanical structure were implemented in this work. As patients in the early

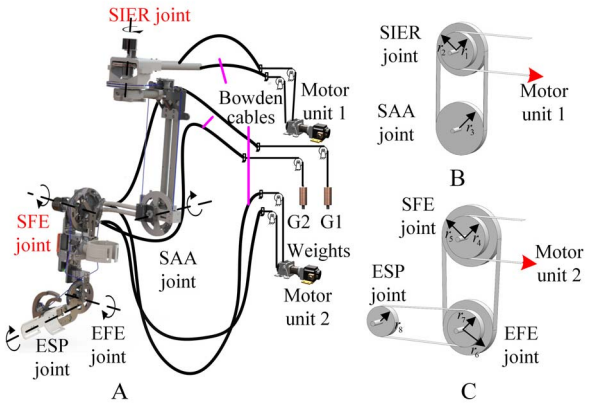

Fig. 2. The robotic mechanism to replicate the synergic feature. A. CAD model of the Armule exoskeleton robot mechanical system. Two active joints (red), three coupling joints (black). The active joints are connected to the actuator and coupled to the passive joints at a specific transmission ratio to reproduce the coupling matrix. The coupling mechanism of the actuated joints: (B) SIER and SAA joints in cluster one. Specifically, $r_1 = 50mm$, $r_2 = 66mm$ and $r_3 = 75mm$; (C) SFE, EFE and ESP joints in cluster two. Specifically, $r_4 = 50mm$, $r_5 = 74mm$, $r_6 = 56mm$, $r_7 = 37mm$ and $r_8 = 74mm$.

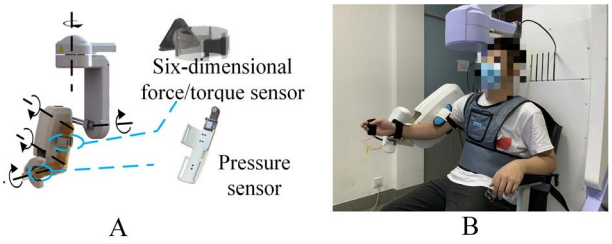

Fig. 3. A: Pressure sensors and six-dimensional force/torque sensors were installed in the linkage cuffs of the forearm and upper arm, respectively, which were used to estimate the patient's motion intention. B: Participant was training with the Armule exoskeleton robot.

stage of rehabilitation treatment are typically unable to move their distal joints to apply high enough interaction forces to the handle to trigger the sensor. We removed the handle and updated the mechanical design of the linkage cuffs, as shown in Fig. 3.A. The wrist joints were instead fixed in the forearm linkage cuff. Pressure sensors and six-dimensional force/torque sensors were installed in the linkage cuffs of the forearm and upper arm, respectively, to estimate the patient's motion intention.

B. Semitransparent Active Control Strategy

To generate assistive movements similar to natural reaching movements in response to the user's motion intentions, building on previous work [49], Admittance control in joint space is proposed. We detected the interaction forces between the patient and the linkage cuffs to determine the patient's subjective movement intention. The interaction forces were converted to the command speed in the joint space with an admittance control method. The actuator velocities were then obtained by their projection in the two-dimensional manifold in the drive space.

$$\begin{aligned} \boldsymbol{V}_D &= \boldsymbol{P}\boldsymbol{A}\boldsymbol{J}^T\left({}^T_u\boldsymbol{T}\left(\boldsymbol{F}^u - {}^0_u\boldsymbol{T}\hat{\boldsymbol{G}}_u\right) + {}^T_f\boldsymbol{T}\left(\boldsymbol{F}^f - {}^0_f\boldsymbol{T}\hat{\boldsymbol{G}}_f\right)\right) \\ \boldsymbol{P} &= \left(\boldsymbol{C}^T\boldsymbol{C}\right)^{-1}\boldsymbol{C}^T \end{aligned} \tag{2}$$

where $\boldsymbol{V}_D = \dot{\boldsymbol{u}}_t \in \mathbb{R}^2$ is the actuator velocity vector, $\boldsymbol{J}$ is the Jacobian matrix of the exoskeleton, ${}^T_u\boldsymbol{T}$ and ${}^T_f\boldsymbol{T}$ are the adjoin matrices of the upper arm and forearm to the end of the exoskeleton respectively. ${}^0_u\boldsymbol{T}$ and ${}^0_f\boldsymbol{T}$ are the adjoin matrices of the upper arm and forearm to space basis coordinates respectively. $\boldsymbol{F}^u$ and $\boldsymbol{F}^f$ are the force vectors detected in the upper arm and forearm respectively. $\hat{\boldsymbol{G}}_u$ and $\hat{\boldsymbol{G}}_f$ are the gravity compensation value estimated in real-time for the upper arm and forearm respectively. $\boldsymbol{A} \in \mathbb{R}^{5\times5}$ is admittance matrix that takes the form: $\boldsymbol{A} = \left[\alpha I_{5\times5}\right]$, where $\alpha > 0$ is the admittance coefficient. The larger this coefficient is, the smaller the torque is needed to generate the same motion. As the interaction force on the exoskeleton is determined by the user's voluntary action, the value of $\boldsymbol{A}$ may be arbitrarily taken in $\mathbb{R}^{5\times5}$. After repeated tests and adjustments, the initial value of the parameter was set to be $\alpha = 0.05rad/(s \cdot N \cdot m)$, this parameter can be adjusted according to the requirements of the patients and therapists. Because of the coupling mechanism, the five-dimensional joint command velocity generated by the joint space admittance controller can be projected into the drive two-dimensional subspace through the projection matrix $\boldsymbol{P}$ to obtain the actuator velocity $\boldsymbol{V}_D$.

When this control strategy was used, each participant was required to move his hand towards the target and apply interaction force to the linkage cuffs naturally. Once the force is detected, the controller calculates the torque required for each joint and uses the admittance coefficient to convert it into velocity, then, the actuator is commanded to produce the motion closest to the movement intention. Enclosed by the exoskeletal robot, the subject's arm will be continuously corrected until his hand reached various targets. Because the exoskeleton drive operates in speed mode, And it's always been $u_t = \int_0^t V_D dt$. This means that the exoskeleton can maintain a coordinated motion pattern all the time.

Under such a control strategy, the exoskeleton can drive the arm and the exoskeleton according to the patient's perceived subjective movement intention. Since the rehabilitation robot can only produce anthropomorphic motions derived from the linear combination of synergy primitives, the calculated movement intention of the patient might be inconsistent with the actual movement direction of the robot. In general, the magnitude of the deviation is related to the operating point and the direction of the applied force, which is determined by the subspace projection formula (as shown in Fig. 4). The rehabilitation robot can be easily driven only when the patient's movement intention is similar to the human natural movement characteristics. We believe that this kind of control strategy is not entirely transparent, which can help suppress pathological movement patterns and induce patients to relearn normal postural synergy without causing severe discomfort, and we call it as a semitransparent active control strategy.

C. Weight Compensation

The exoskeleton in this study adopts both a mechanical structure that provided weight compensation and a dynamic-based weight compensation algorithm to offset the gravity of the robotic arm and patient's arm. Thus, the patient's ability to generate residual motion can be improved, enabling

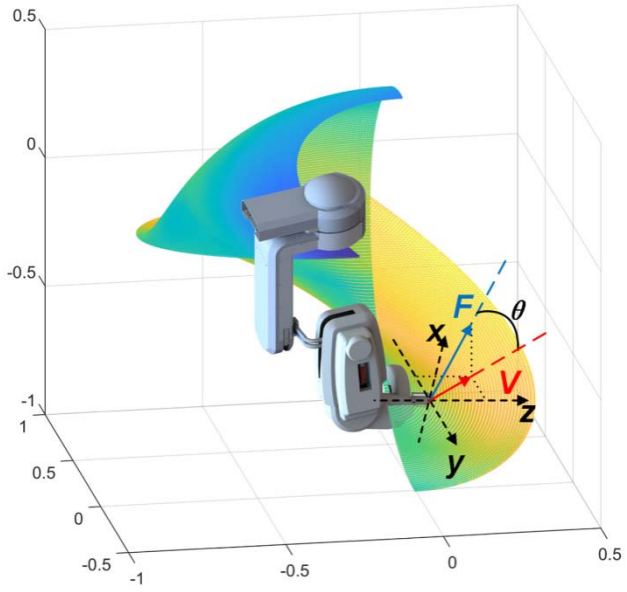

Fig. 4. The calculated movement intention of the patient might be inconsistent with the actual movement direction of the exoskeleton. The surface represents the workspace of the exoskeleton. $\boldsymbol{F}$ is the equivalent interaction force at the end of the exoskeleton, which was taken as the patient's motion intention. $\boldsymbol{V}$ is the actual velocity vector of exoskeleton in workspace. The Angle between $\boldsymbol{F}$ and $\boldsymbol{V}$ is θ, which will be used for calculating intent response rate later in this article.

the training of active reaching movements [50]. When in operation, the mechanical weight compensation structure applies the appropriate torques to the actuated joints to balance the arm's weight and reduce the burden of the motor unit. On the other hand, the exoskeleton compensates for the patient's arm weight in the control system using a dynamic model-based approach. Six-dimensional force/torque sensor data is used to estimate the patient's arm weight when the patient is in the passive training mode and compensate during the active training mode to eliminate the influence of the patient's arm weight on the process of determining the user's motion intention. The compensation coefficient can be adjusted in the human-computer interaction interface.

The measured values of the six-dimensional force and torque sensor when the patient is in the passive training mode are $\boldsymbol{F}_u^{\text{mes}}$ and $\boldsymbol{F}_f^{\text{mes}}$, respectively. It takes n samples ($n > 2$). Gravity compensation $\hat{\boldsymbol{G}}$ can be calculated as follow:

$$\hat{\boldsymbol{G}} = \left(\boldsymbol{W}^{\mathrm{T}}\boldsymbol{W}\right)^{-1}\boldsymbol{W}^{T}\boldsymbol{\omega}\boldsymbol{b} \tag{3}$$

where $\boldsymbol{W} = [{}^0\boldsymbol{T}_1, \ldots, {}^0\boldsymbol{T}_n]^T$, b $= [\boldsymbol{F}_1^{\text{mes}}, \ldots, \boldsymbol{F}_n^{\text{mes}}]^T$, $\boldsymbol{\omega}$ is the compensation coefficient.

D. Rehabilitation Training Application

We designed a human-computer interface to guide patients to participate in the training. In general, training can be divided into two categories, passive mode, and active mode.

In the passive mode, the rehabilitation exoskeleton guides the patient to perform natural reaching movements designed and recorded by therapists. When the rehabilitation robot is in

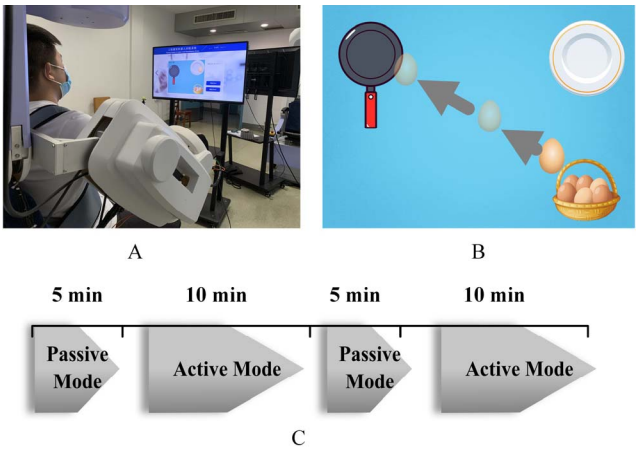

Fig. 5. A: The exoskeleton calculates and assists the patient in performing the natural reaching movement. B: The frying eggs task, there is visual feedback during training to indicate the direction of the patient's exercise efforts. The participants were asked to perform two sets of exercises per session. Each set consisted of 5 minutes of passive training and 10 minutes of active training.

the active mode, the exoskeleton will calculate and assist the patient in performing the natural reaching movement closest to the patient's intention based on the motion tendencies of the whole arm. In this phase, the robotic exoskeleton detects patients' intentions and assists patients in achieving anthropomorphic movements as well as ADL-related tasks with virtual games, such as shooting targets, playing whack-a-mole, drinking water, wiping the face, cleaning a window, and frying eggs (Fig. 5 A,B). The rotation angles of the two active joints are associated with the position of the operating objects in the virtual environment, with a fixed mapping relationship. Two active synergy primitives drive the exoskeleton, and the patient can see the corresponding information on a screen. The exoskeleton guides patients with visual cues and provides feedback to complete tasks involving anthropomorphic postures and trajectories.

III. Experiments

A. Participants

In order to test the feasibility of the exoskeleton for upper limb rehabilitation, 8 participants (age, 47.0 ± 9.9 years; time since stroke, 70.1 ± 47.7 days; see TABLE I) were enrolled in the study. The inclusion criteria were as follows: (1) an age of 18-80 years; (2) a clinical diagnosis of the first-ever stroke within 6 months before enrollment; and (3) upper limb hemiplegia, defined as a score between 8 and 47 on the FMA-UE. The exclusion criteria were as follows: (1) an orthopedic condition of the upper limb, e.g., fixed contracture, shoulder subluxation, severe arthritis, or recent fracture; and (2) severe cognitive defects or aphasia hindering the patient's ability to understand or follow instructions. All the participants signed informed consent forms in accordance with the latest version of the Declaration of Helsinki. The Clinical Trials Ethics Committee of Huazhong University of Science and Technology granted ethical approval for this study (certificate number IRB [2018]-235).

TABLE I
PARTICIPANT CHARACTERISTICS

Subjects ID	Gender (M/F)	Age (years)	Days between onset and enrollment	Stroke type (H/I)	NIHSS	Paretic side (L/R)	FMA-UE	MMSE
1	M	43	100	H	5	L	25	24
2	M	65	97	I	2	L	32	30
3	M	45	152	H	4	L	36	27
4	M	38	94	H	6	R	9	25
5	M	48	16	H	7	L	8	29
6	M	33	42	I	2	R	60	30
7	M	49	24	I	6	L	21	25
8	M	55	36	I	6	L	8	24

M, Male; H, Hemorrhagic; I, Ischemic; L, Left; R, Right; MMSE, mini-mental state examination (range 0-30).

B. Setup and Data Recording

Demographic information, stroke type, time since stroke onset, mini-mental state examination (MMSE) scores were collected at baseline. The clinical outcome measures were assessed at baseline and immediately after the 4-week intervention. To avoid assessment bias, an independent evaluator blinded to the study procedure completed all the outcome measures. The participants were asked to sit in a chair with a backrest in front of the exoskeleton, and their torsos were secured with chest straps to prevent compensatory movements. The upper limbs were initially held in a natural, relaxed position. The exoskeleton attachments were adjusted according to the length and circumference of each patient's upper limb.

Throughout the training period, the sensors on the exoskeleton monitored the kinematics and interactive forces, which were sampled at 100 Hz and stored in text format, including angle-time data of five joints and force-time data fed back by two force sensors. Then, the data were extracted through a semiautomatic custom program in MATLAB software (version 2018A, The MathWorks, Natick, Massachusetts, USA.) to analyze the kinematics and human-robot interaction indicators.

C. Protocol

The participants received task-specific training involving 5-DOF movements of the upper extremity in a 3-dimensional workspace assisted by the exoskeleton, 45 minutes daily, 5 days/week for 4 weeks (total of 20 sessions). The participants were asked to perform two sets of exercises per session. Each set consisted of 5 minutes of passive training and 10 minutes of active training (Fig. 5C).

D. Outcome Measures

1) Clinical Outcome Measurements: The primary outcome was the FMA-UE score, which reflected the severity of the participants' upper extremity motor impairments. The secondary outcomes were the ARAT score, which reflected upper limb performance, especially the hand's fine motor function, and the mBI score, which reflected the patient's level of functional independence in ADL. In addition, we designed two 10-point Likert scales (LSs), measuring the subjects' perception of their level of enjoyment and degree of improvement [51] (see TABLE II, III).

TABLE II
10-POINT LIKERT SCALE FOR SUBJECTIVE ENJOYMENT

Circle the number that best describes your feelings about the type of therapy you got for your arm **Satisfaction Level (range 1-10)**									
1	2	3	4	5	6	7	8	9	10
None									Very much

TABLE III
10-POINT LIKERT SCALE FOR SUBJECTIVE IMPROVEMENT

Circle the number that best describes how much you feel your arm has gotten better **Self-Perception of Improvement (range 1-10)**									
1	2	3	4	5	6	7	8	9	10
None									Very much

2) Measurements With the Exoskeleton: In this paper, we used four indicators measured by the robot to evaluate the motion control ability of the patients with the assistance of the robot. We previously recorded exercise data from 10 healthy individuals performing the same task using the exoskeleton for reference. To eliminate the interference of different tasks, the patients were asked to complete five reaching movement tasks (frying eggs) in a virtual reality environment for each active training phase. For this training task, they put a virtual raw egg into a pan on the screen. The participants were verbally encouraged to do their best to complete the task at their preferred speed.

Motion Smoothness in the Workspace S_w: This parameter indicates whether the patient's joint trajectories are mixed with other submovements. The extent of S_w during the reaching movement was characterized by path jerk, the third derivative of the joint angle of the patients. The smaller the jerk was, the smoother the trajectory.

$$S_w = \frac{1}{T}\sum_{t=1}^{T} \|\dddot{s}\|_F \tag{4}$$

where s is the position of the end of the exoskeleton in the workspace, T is the normalized time parameter.

Position Error P_e: This measure indicates the deviation between the actual joint position and the anthropomorphic

TABLE IV
EXOSKELETON KINEMATIC AND INTERACTION FORCE METRICS

Kinematic/interaction force metrics	Pre-treatment	Post-treatment	Within-Group Differences	*p* Value
S_w	17.22±6.99	6.69±3.49	7.22±2.55	0.004 **
P_e	465.33±128.64	341.87±171.95	107.54±38.02	0.014 *
R_i	0.17±0.04	0.22±0.06	0.04±0.01	0.008 **

Values are presented as means ± standard deviations. *: p<0.05; **: p<0.01

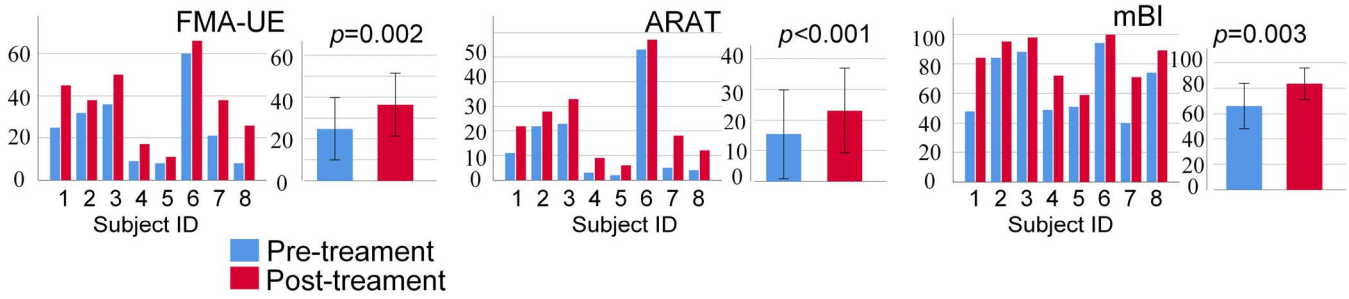

Fig. 6. Clinical outcomes, the primary outcome was the FMA-UE score, the secondary outcomes were the ARAT score and the mBI score.

joint position over the whole trajectory. It is defined as the covariance distance between the patient's trajectories and the healthy person in two synergy basis directions when the subjects performed the same training task. The movements generated by this exoskeleton are the linear superposition of two principal motion components. During the training process, users can freely combine these two principal motion components, so as to gradually approach the movement target. The coefficient was high at the segments with low covariance to punish high postural deviations. In the segments with high covariance, the coefficient is lower, because healthy people also have more posture variation in these segments. The smaller the P_e value, the more similar the trajectory of patients and healthy people.

$$P_e = \frac{1}{T}\sum_{t=1}^{T}\sqrt{\left(\mathbf{S}_t - \overline{\boldsymbol{\mu}}_t\right)^T \boldsymbol{\Sigma}_t^{-1}\left(\mathbf{S}_t - \overline{\boldsymbol{\mu}}_t\right)} \tag{5}$$

where $\mathbf{S}_t$ is the active joint position at t, $\overline{\boldsymbol{\mu}}_t$ is the mean active joint positions for healthy people at t, $\boldsymbol{\Sigma}_t$ is the covariance matrix of active joint position of healthy people at t.

Intent response rate R_i: This parameter was defined as the cosine of the angle between the direction of the subject's intention to move, i.e., the direction of equivalent end interaction force, and the actual direction in which the exoskeleton moved. This measure reflects the extent to which the subject's movement intentions are executed by the exoskeleton.

$$R_i = \cos(\theta) = \frac{\mathbf{F}\cdot\mathbf{V}}{\|\mathbf{F}\|\cdot\|\mathbf{V}\|} \tag{6}$$

where $F \in \mathbb{R}^6 V \in \mathbb{R}^6$. According to the definition $R_i \in (0, 1)$. The closer to zero R_i is, the more exoskeleton assists the participant. The closer to 1 R_i is, the more similar the movement of the exoskeleton is to the patient's movement intention.

TABLE V
DEGREE OF GENERAL SUBJECTIVE SATISFACTION

Subjects ID	Satisfaction Level (range 1-10)	Self-Perception of Improvement (range 1-10)
1	9	10
2	8	9
3	8	10
4	10	9
5	9	10
6	10	10
7	10	10
8	8	8

E. Statistical Analysis

Statistical analyses were performed using SPSS software (version 26.0, IBM Corporation, Chicago, IL, USA). To assess the normality of the quantitative data, the Shapiro-Wilk test was used. The baseline data were compared using independent-samples t-tests (for continuous variables) and Fisher's exact tests (for categorical variables). Before and after the intervention, differences were compared using paired t-tests (for normally distributed data) and Wilcoxon signed-rank tests (for nonparametric equivalent tests). For all the statistical tests conducted, a two-sided p-value of less than 0.05 was considered significant.

IV. RESULTS

Overall, the exoskeleton showed high levels of safety and satisfaction (TABLE V). Obtained results also demonstrate the large enthusiasm of subjects, but these results are only preliminary due to the limited number of subjects.

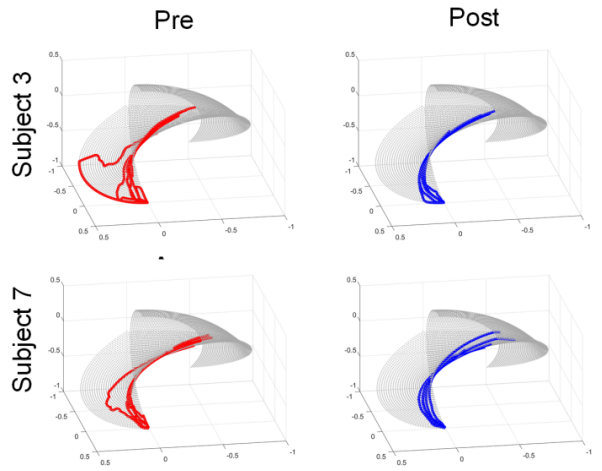

Fig. 7. Two exemplar subjects' performance in the reaching tasks pre-treatment and post-treatment. The four panels represent the curves of the exoskeleton end trajectory in workspace during the time-normalized tasks. As shown in the panels, the end trajectory in post-treatment(blue) are smoother and more focused than the end trajectory in pre-treatment(red).

At 4 weeks, the patients trained showed significant reductions in motor impairment (see Fig. 6) and significant improvements in motor capacity, as measured by the FMA-UE (difference, 11.50 ± 6.50 points; 95% confidence interval [CI], 6.06 to 16.94; $p = 0.002$), the minimal clinically important difference (MCID) for FMA-UE is 4 points in acute to subacute stroke and 5.25points in chronic stroke. The difference in motor impairment recovery was greater than the MCID value. The ARAT (difference, 7.75 ± 3.33 points; 95% confidence interval [CI], 4.97 to 10.53; p <0.001) the MCID for the ARAT in stroke individuals is 10% of its range (5.7 points). The difference was greater than the MCID value; and the mBI (difference, 17.50 ± 11.22 points; 95% confidence interval [CI], 8.12 to 26.88; $p = 0.003$). The MCID for the mBI in stroke individuals is 1.85 points. The difference was greater than the MCID value.

Fig. 7 shows two examples of subjects' performance in the reaching tasks pretreatment and post-treatment. The patients showed significant improvements in motion smoothness in the joint space (difference, 7.22 ± 2.55; $p = 0.004$), postural synergy error (difference, 107.54 ± 38.02; $p = 0.014$), and the intent response rate (difference, 0.04 ± 0.01; $p = 0.008$) after the 4-week intervention (see TABLE IV).

V. Discussion

We developed a postural synergy-based exoskeleton, the Armule, to provide natural human movement training for stroke patients. Armule has five degrees of freedom to provide motion assistance for the shoulder and elbow. Eight stroke patients used this exoskeleton and underwent evaluations. Our preliminary test results showed that in general, the 4 weeks of therapy was acceptable and feasible in post-stroke upper limb rehabilitation. The Armule was successful in assisting stroke patients with rehabilitation training, and the subjects responded well to the exoskeleton, without adverse reactions related to the exoskeleton.

A. Clinical Outcome Measurements

According to the clinical scale outcomes, after 4 weeks of the intervention, all subjects showed significant improvements in the clinical outcomes, which reduced upper extremity motor impairment by 11.50 FMA-UE points (MCID: 4 points for acute to subacute stroke and 5.25points for chronic stroke), improved the arm motor capacity by 7.75 ARAT points (MCID: 5.7 points) and improved activities of daily living by 8.7 mBI points (MCID: 1.85 points), and optimized kinematic performance. Specifically, the FMA-UE is a highly reliable and valid tool to assess post-stroke motor impairment, which is explicitly rating the quality of movements and abnormal synergies; the ARAT evaluates 19 tests of arm functional capacity, consisting of four subscales: grasp, grip, pinch, and gross movement; and the mBI examines the independence level in basic activities of living (ADL). The mean gain in all of these three assessments over the whole course of the study higher than the MCID values, and despite the limited sample size and lack of a control group, the Armule shows great potential for improving upper extremity motor impairment, functional capacity, activities of daily living.

In the previous exoskeleton studies, Klamroth-Marganska *et al.* employed ARMin and found that individuals showed significant improvements in motor function, spasticity, and function in daily life [52]. In this study, patients with chronic impairment after stroke were included; Training was set to be three times a week in the for a period of 8 weeks (total 24 sessions), and the minimum time for each session was 45 min, which implies that the training intensity and duration is slightly higher than in our study. Although our study has made greater improvement in FMA-UE score, the superiority of our study needs to be further studied due to the lack of control group and small clinical scale of our study, and it should be admitted that the patients included in our study were in the subacute phase, suggesting a certain degree of spontaneous recovery. In addition, their study found that patients assigned to robotic therapy gained motor function faster, but could not fully consolidate the achievements when the therapy ceased. Therefore, the training intensity and duration of our robot therapy also need to be further explored in subsequent studies. In contrast, a meta-analysis produced conflicting results. This Meta-analysis suggests that robotic therapy showed significant but small improvements in motor control, no effects were found for upper limb capacity and basic ADL [53]. Since our proposed exoskeleton uses a completely different approach to structural design and control, we believe our proposed exoskeleton may have a positive impact, despite our results are preliminary and lack a control group. The exoskeleton that we proposed can provide therapy incorporating meaningful tasks, including drinking water, wiping their face, cleaning a window, and frying eggs. The tasks were well matched with human-like movements because participants may not learn how to use the paretic arm and apply the improvements in real life without the context-related task practice [54]. Movements of the upper extremities required multi-DOF motion in three-dimensional space, while games are generally planar on the screen and incompatible with the actual scenarios [55]. The postural

synergy-design adopted by our proposed exoskeleton just decomposes the complex tasks in the workspace into two principal component movements, and maps the synthesis of the two principal movements on the screen to indicate the direction of the patient's efforts. Under the visual guidance and feedback, the participant could complete multi-DOF anthropomorphic tasks within the dimension reduction subspace, that is, the desired endpoint trajectories in the virtual game. Some recent studies have shown that postural synergies with visual feedback might improve the efficiency of motor learning in healthy people [46], [47]. We believed such simulated tasks per se and visual feedback might induce much "real" activity-related sensorimotor input to enhance upper limb motor recovery and generalize it to real-world function, which deserves further investigation.

B. Measurements With the Exoskeleton

According to the kinematic data analysis, after the 4-week intervention, the stroke subjects were able to complete specific tasks with the assistance of the exoskeleton and keep the movements being performed similarly to those of healthy people and the smoothness. This confirms the adaptability study by Brokaw *et al.* [56] in which synchronous shoulder abduction and elbow extension were practice using ARMin III. They speculate that with longer bouts of training, increased movement smoothness may emerge. The same findings were reported by Frisoli using L-Exos [13]. Our finding suggested that pathological synergy and tremors might be reduced after natural human movement training. Crocher *et al.* [44] quantify the synergies imposed by the therapist as a natural constraint and impose this constraint during rehabilitation using the ABLE exoskeleton. Their results suggest that the constraint may push the coordination of the movement in the direction desired by the therapist, in general agreement with our study.

The intention response rate results show that our exoskeleton can always perform the corresponding movements in response to the patient's intention to a certain extent. As the rehabilitation progressed, the rate of intention response increased; this suggests a decrease in pathological synergistic or compensatory motor effects. Although all patients showed improvement in the interaction rate, the absolute magnitude of improvement was small, which was speculated to be related to the degree of muscle strength recovery in stroke patients.

C. Comparison to Related Work

Compared with previous exoskeleton rehabilitation robots, this rehabilitation robot has the following characteristics.

In the previous works [42], [49], the self-reaching movements of healthy volunteers are analyzed by the PCA method and extracted the above postural synergies, which can account for more than 80% of the natural movement variation. Since postural synergies of upper limb self-reaching movements were embedded in this exoskeleton's structure, the motions generated by the exoskeleton were in line with the natural movement characteristics of the human upper limb. It's not the same as previous studies that reproduce kinematic synergy at the control level [11], [30], [44], [56], [57], to our knowledge, this is the first clinical trial of an upper exoskeleton that integrates postural synergy into the mechanical structure for the rehabilitation of patients with chronic stroke. All subjects showed significant improvements in the clinical outcomes, which indicated that using the postural synergy-based exoskeleton for rehabilitation training is safe and feasible.

Our control strategy identified patients' movement intention and facilitated patients to actively participate in functional exercise training by using the admittance control method in the dimension reduction subspace. And unlike previous exoskeleton rehabilitation robots, the incomplete transparent control strategy limited the patients' pathological synergy movements and encouraged them to perform natural movements. In addition, we provided visual feedback during training to indicate the direction of the patient's efforts. Patients are encouraged to use a combination of active exercise components close to those of healthy to reproduce the natural human movement, which may have helped accelerate motor function restoration in the patients [46]. The safety and satisfaction questionnaire showed that the non-transparent control strategy we adopted did not cause patient discomfort.

A recent robot-assisted training randomized controlled trial using the MIT-Manus robotic gym system for the upper limb after stroke reported that, on average, robot-assisted training was more costly than both enhanced therapy and usual care, and the robot-assisted training was not a cost-effective treatment for the National Health Service [58]. This might be a common problem of rehabilitation robots at present, which seriously restricts the promotion and application of robot-assisted rehabilitation. Our exoskeleton included a mechanical structure and control algorithm that compensated for gravity and friction, significantly improving the equipment's Backdriveability and the patient's ability to participate in training actively. In this way, the whole rehabilitation exoskeleton robot can be driven by only two active motors, which reduces the hardware cost and improves the possibility of equipment promotion.

D. Limitations

In this study, there are some limitations worth noting. First, the small sample of participants may limit the generalizability of our findings in terms of efficacy, despite the included patients having statistically significant improvements. Therefore, larger randomized controlled trials that include subjects with heterogeneous characteristics should be conducted to confirm the study results. Second, the relationships between the clinical improvements and robot test indicators need to be more carefully researched and explained. We plan to conduct larger studies to assess the correlations between the robot test index and clinical improvements and adopt motion capture technology and functional magnetic resonance imaging to uncover the evolution of the underlying motor synergies and neural mechanisms of motor performance improvement in stroke patients. Third, this exoskeleton generates motions by a linear combination of postural synergy primitives extracted from 5 self-reaching movements; thus, this exoskeleton only focuses on self-care activities and involves limited movements. In the future, we need to include more movement template

libraries to expand the training task types of rehabilitation exoskeletons.

VI. Conclusion

This paper describes a postural synergy-based exoskeleton, Armule, to provide natural human movement training for stroke patients. Our preliminary study shows that the subjects are well adapted to our device, assisting the subjects in completing functional movements with the natural human movement characteristics. The preliminary clinical intervention results indicate that the postural synergy-based exoskeleton improved the subjects' motor control and their upper limbs' ADL function.

References

[1] S. I. Hay *et al.*, "Global, regional, and national disability-adjusted life-years (DALYs) for 333 diseases and injuries and healthy life expectancy (HALE) for 195 countries and territories, 1990–2016: A systematic analysis for the Global Burden of Disease Study 2016," *Lancet*, vol. 390, no. 10100, pp. 1260–1344, 2017.

[2] S. J. Albert and J. Kesselring, "Neurorehabilitation of stroke," *J. Neurol.*, vol. 259, pp. 817–832, May 2012.

[3] L. M. Muratori, E. M. Lamberg, L. Quinn, and S. V. Duff, "Applying principles of motor learning and control to upper extremity rehabilitation," *J. Hand Therapy*, vol. 26, no. 2, pp. 94–102, May Jun. 2013.

[4] C. M. Butefisch *et al.*, "Mechanisms of use-dependent plasticity in the human motor cortex," *Proc. Nat. Acad. Sci. USA*, vol. 97, no. 7, pp. 3661–3665, Mar. 2000.

[5] V. S. Huang, A. Haith, P. Mazzoni, and J. W. Krakauer, "Rethinking motor learning and savings in adaptation paradigms: Model-free memory for successful actions combines with internal models," *Neuron*, vol. 70, no. 4, pp. 787–801, May 2011.

[6] D. J. Reinkensmeyer, J. L. Emken, and S. C. Cramer, "Robotics, motor learning, and neurologic recovery," *Annu. Rev. Biomed. Eng.*, vol. 6, no. 1, pp. 497–525, Aug. 2004.

[7] M. Coscia *et al.*, "Neurotechnology-aided interventions for upper limb motor rehabilitation in severe chronic stroke," *Brain*, vol. 142, no. 8, pp. 2182–2197, Aug. 2019.

[8] L. Oujamaa, I. Relave, J. Froger, D. Mottet, and J. Y. Pelissier, "Rehabilitation of arm function after stroke. Literature review," *Ann. Phys. Rehabil. Med.*, vol. 52, no. 3, pp. 269–293, Apr. 2009.

[9] H. S. Lo and S. Q. Xie, "Exoskeleton robots for upper-limb rehabilitation: State of the art and future prospects," *Med. Eng. Phys.*, vol. 34, no. 3, pp. 261–268, Apr. 2012.

[10] R. A. R. C. Gopura, D. S. V. Bandara, K. Kiguchi, and G. K. I. Mann, "Developments in hardware systems of active upper-limb exoskeleton robots: A review," *Robot. Auton. Syst.*, vol. 75, pp. 203–220, Jan. 2016.

[11] T. Proietti, E. Guigon, A. Roby-Brami, and N. Jarrassé, "Modifying upper-limb inter-joint coordination in healthy subjects by training with a robotic exoskeleton," *J. NeuroEng. Rehabil.*, vol. 14, no. 1, p. 55, Jun. 2017.

[12] E. Pirondini *et al.*, "Evaluation of the effects of the arm light exoskeleton on movement execution and muscle activities: A pilot study on healthy subjects," *J. NeuroEng. Rehabil.*, vol. 13, no. 1, pp. 1–21, Jan. 2016.

[13] A. Frisoli *et al.*, "Positive effects of robotic exoskeleton training of upper limb reaching movements after stroke," *J. NeuroEng. Rehabil.*, vol. 9, no. 1, p. 36, 2012.

[14] J. C. Perry, J. Rosen, and S. Burns, "Upper-limb powered exoskeleton design," *IEEE/ASME Trans. Mechatronics*, vol. 12, no. 4, pp. 408–417, Aug. 2007.

[15] F. Just, K. Baur, R. Riener, V. Klamroth-Marganska, and G. Rauter, "Online adaptive compensation of the ARMin rehabilitation robot," in *Proc. 6th IEEE Int. Conf. Biomed. Robot. Biomechatronics (BioRob)*, Jun. 2016, pp. 747–752.

[16] B. Kim and A. D. Deshpande, "An upper-body rehabilitation exoskeleton harmony with an anatomical shoulder mechanism: Design, modeling, control, and performance evaluation," *Int. J. Robot. Res.*, vol. 36, no. 4, pp. 414–435, 2017.

[17] C. Carignan, J. Tang, and S. Roderick, "Development of an exoskeleton haptic interface for virtual task training," in *Proc. IEEE/RSJ Int. Conf. Intell. Robots Syst.*, Oct. 2009, pp. 3697–3702.

[18] A. Otten, C. Voort, A. Stienen, R. Aarts, E. van Asseldonk, and H. van der Kooij, "LIMPACT: A hydraulically powered self-aligning upper limb exoskeleton," *IEEE/ASME Trans. Mechatronics*, vol. 20, no. 5, pp. 2285–2298, Oct. 2015.

[19] Y. Zimmermann, A. Forino, R. Riener, and M. Hutter, "ANYexo: A versatile and dynamic upper-limb rehabilitation robot," *IEEE Robot. Autom. Lett.*, vol. 4, no. 4, pp. 3649–3656, Oct. 2019.

[20] C. Shirota *et al.*, "On the assessment of coordination between upper extremities: Towards a common language between rehabilitation engineers, clinicians and neuroscientists," *J. NeuroEng. Rehabil.*, vol. 13, no. 1, pp. 1–14, Sep. 2016.

[21] M. Guidali, A. Duschau-Wicke, S. Broggi, V. Klamroth-Marganska, T. Nef, and R. Riener, "A robotic system to train activities of daily living in a virtual environment," *Med. Biol. Eng. Comput.*, vol. 49, no. 10, pp. 1213–1223, Oct. 2011.

[22] A. L. Wong, A. M. Haith, and J. W. Krakauer, "Motor planning," *Neuroscientist*, vol. 21, no. 4, pp. 385–398, 2015.

[23] N. Jarrasse and G. Morel, "Connecting a human limb to an exoskeleton," *IEEE Trans. Robot.*, vol. 28, no. 3, pp. 697–709, Jun. 2012.

[24] N. S. Makowski, J. S. Knutson, J. Chae, and P. E. Crago, "Control of robotic assistance using poststroke residual voluntary effort," *IEEE Trans. Neural Syst. Rehabil. Eng.*, vol. 23, no. 2, pp. 221–231, Mar. 2015.

[25] G. Tacchino, M. Gandolla, S. Coelli, R. Barbieri, A. Pedrocchi, and A. M. Bianchi, "EEG analysis during active and assisted repetitive movements: Evidence for differences in neural engagement," *IEEE Trans. Neural Syst. Rehabil. Eng.*, vol. 25, no. 6, pp. 761–771, Jun. 2017.

[26] M. Mihara *et al.*, "Near-infrared spectroscopy-mediated neurofeedback enhances efficacy of motor imagery-based training in poststroke victims a pilot study," *Stroke*, vol. 44, no. 4, p. 1091, Apr. 2013.

[27] D. Borton, S. Micera, J. D. R. Millán, and G. J. S. T. M. Courtine, "Personalized neuroprosthetics," *Sci. Transl. Med.*, vol. 5, no. 210, 2013, Art. no. 210rv2.

[28] A. Sawers and L. H. Ting, "Perspectives on human-human sensorimotor interactions for the design of rehabilitation robots," *J. NeuroEng. Rehabil.*, vol. 11, no. 1, p. 142, 2014.

[29] N. Hogan and H. I. Krebs, "Interactive robots for neuro-rehabilitation," *Restorative Neurol. Neurosci.*, vol. 22, no. 3, pp. 349–358, 2004.

[30] N. Jarrassé *et al.*, "Robotic exoskeletons: A perspective for the rehabilitation of arm coordination in stroke patients," *Frontiers Hum. Neurosci.*, vol. 8, p. 947, Dec. 2014.

[31] A. A. Blank, J. A. French, A. U. Pehlivan, and M. K. O'Malley, "Current trends in robot-assisted upper-limb stroke rehabilitation: Promoting patient engagement in therapy," *Current Phys. Med. Rehabil. Rep.*, vol. 2, no. 3, pp. 184–195, Sep. 2014.

[32] N. Rehmat, Z. Jie, Q. Liu, S. Q. Xie, H. Liang, and M. Wei, "Upper limb rehabilitation using robotic exoskeleton systems: A systematic review," *Int. J. Intell. Robot. Appl.*, vol. 2, no. 3, pp. 283–295, Sep. 2018.

[33] V. L. S. Profeta and M. T. Turvey, "Bernstein's levels of movement construction: A contemporary perspective," *Hum. Movement Sci.*, vol. 57, pp. 111–133, Feb. 2018.

[34] M. Bruton and N. O'Dwyer, "Synergies in coordination: A comprehensive overview of neural, computational, and behavioral approaches," *J. Neurophysiol.*, vol. 120, no. 6, pp. 2761–2774, Dec. 2018.

[35] S. Marco *et al.*, "Hand synergies: Integration of robotics and neuroscience for understanding the control of biological and artificial hands," *Phys. Life Rev.*, vol. 17, pp. 1–23, Jul. 2016.

[36] G. Averta, C. D. Santina, G. Valenza, A. Bicchi, and M. Bianchi, "Exploiting upper-limb functional principal components for human-like motion generation of anthropomorphic robots," *J. NeuroEng. Rehabil.*, vol. 17, no. 1, pp. 1–15, May 2020.

[37] G. Averta, C. D. Santina, E. Battaglia, F. Felici, M. Bianchi, and A. Bicchi, "Unvealing the principal modes of human upper limb movements through functional analysis," *Frontiers Robot. AI*, vol. 4, p. 37, Aug. 2017.

[38] Y. Hashiguchi *et al.*, "Merging and fractionation of muscle synergy indicate the recovery process in patients with hemiplegia: The first study of patients after subacute stroke," *Neural Plasticity*, vol. 2016, pp. 1–7, Oct. 2016.

[39] A. Sarasola-Sanz *et al.*, "Design and effectiveness evaluation of mirror myoelectric interfaces: A novel method to restore movement in hemiplegic patients," *Sci. Rep.*, vol. 8, no. 1, Nov. 2018, Art. no. 16688.

[40] C. Nam, W. Rong, W. Li, Y. Xie, X. Hu, and Y. Zheng, "The effects of upper-limb training assisted with an electromyography-driven neuromuscular electrical stimulation robotic hand on chronic stroke," *Frontiers Neurol.*, vol. 8, p. 679, Dec. 2017.

[41] V. C. K. Cheung *et al.*, "Muscle synergy patterns as physiological markers of motor cortical damage," *Proc. Nat. Acad. Sci. USA*, vol. 109, pp. 14652–14656, Sep. 2012.
[42] K. Liu, C.-H. Xiong, L. He, W.-B. Chen, and X.-L. Huang, "Postural synergy based design of exoskeleton robot replicating human arm reaching movements," *Robot. Auto. Syst.*, vol. 99, pp. 84–96, Jan. 2018.
[43] S. Tang *et al.*, "Kinematic synergy of multi-DoF movement in upper limb and its application for rehabilitation exoskeleton motion planning," *Frontiers Neurorobotics*, vol. 13, p. 99, Nov. 2019.
[44] V. Crocher, A. Sahbani, J. Robertson, A. Roby-Brami, and G. Morel, "Constraining upper limb synergies of hemiparetic patients using a robotic exoskeleton in the perspective of neuro-rehabilitation," *IEEE Trans. Neural Syst. Rehabil. Eng.*, vol. 20, no. 3, pp. 247–257, May 2012.
[45] M. Hassan *et al.*, "Feasibility of synergy-based exoskeleton robot control in hemiplegia," *IEEE Trans. Neural Syst. Rehabil. Eng.*, vol. 26, no. 6, pp. 1233–1242, Jun. 2018.
[46] K. A. Day and A. J. Bastian, "Providing low-dimensional feedback of a high-dimensional movement allows for improved performance of a skilled walking task," *Sci. Rep.*, vol. 9, no. 1, p. 13, Dec. 2019.
[47] V. Patel, J. Craig, M. Schumacher, M. K. Burns, I. Florescu, and R. Vinjamuri, "Synergy repetition training versus task repetition training in acquiring new skill," *Frontiers Bioeng. Biotechnol.*, vol. 5, p. 9, Feb. 2017.
[48] B. Bobath, "Treatment of adult hemiplegia," *Physiotherapy*, vol. 63, no. 10, pp. 310–313, Oct. 1977.
[49] L. He, C. Xiong, K. Liu, J. Huang, C. He, and W. Chen, "Mechatronic design of a synergetic upper limb exoskeletal robot and wrench-based assistive control," *J. Bionic Eng.*, vol. 15, no. 2, pp. 247–259, Mar. 2018.
[50] F. Just, Ö. Özen, S. Tortora, V. Klamroth-Marganska, R. Riener, and G. Rauter, "Human arm weight compensation in rehabilitation robotics: Efficacy of three distinct methods," *J. NeuroEng. Rehabil.*, vol. 17, no. 1, p. 17, Feb. 2020.
[51] H. A. Abdullah, C. Tarry, C. Lambert, S. Barreca, and B. O. Allen, "Results of clinicians using a therapeutic robotic system in an inpatient stroke rehabilitation unit," *J. NeuroEng. Rehabil.*, vol. 8, no. 1, p. 50, 2011.
[52] V. Klamroth-Marganska *et al.*, "Three-dimensional, task-specific robot therapy of the arm after stroke: A multicentre, parallel-group randomised trial," *Lancet Neurol.*, vol. 13, no. 2, pp. 159–166, 2014.
[53] J. M. Veerbeek *et al.*, "Effects of robot-assisted therapy for the upper limb after stroke: A systematic review and meta-analysis," *Neurorehabil. Neural Repair*, vol. 31, no. 2, pp. 107–121, 2017.
[54] K. A. Almhdawi, V. G. Mathiowetz, M. White, and R. C. delMas, "Efficacy of occupational therapy task-oriented approach in upper extremity post-stroke rehabilitation," *Occupational Therapy Int.*, vol. 23, no. 4, pp. 444–456, Dec. 2016.
[55] A. Basteris, S. M. Nijenhuis, A. H. A. Stienen, J. H. Buurke, G. B. Prange, and F. Amirabdollahian, "Training modalities in robot-mediated upper limb rehabilitation in stroke: A framework for classification based on a systematic review," *J. Neuroeng. Rehabil., Rev.*, vol. 11, p. 111, Jul. 2014.
[56] E. B. Brokaw, R. J. Holley, and P. S. Lum, "Comparison of joint space and end point space robotic training modalities for rehabilitation of interjoint coordination in individuals with moderate to severe impairment from chronic stroke," *IEEE Trans. Neural Syst. Rehabil. Eng.*, vol. 21, no. 5, pp. 787–795, Sep. 2013.
[57] T. Proietti, A. Roby-Brami, and N. Jarrass, "Learning motor coordination under resistive viscous force fields at the joint level with an upper-limb robotic exoskeleton," *Biosyst. Biorobot.*, vol. 15, pp. 1175–1179, Oct. 2016.
[58] H. Rodgers *et al.*, "Robot-assisted training compared with an enhanced upper limb therapy programme and with usual care for upper limb functional limitation after stroke: The RATULS three-group RCT," *Health Technol. Assessment*, vol. 24, no. 54, pp. 1–232, Oct. 2020.